Semi-analytical discontinuous Galerkin finite element method for the calculation of dispersion properties of guided waves in plates

Salah-Eddine Hebaz, Farouk Benmeddour, Emmanuel Moulin, Jamal Assaad

Semi-analytical discontinuous Galerkin finite element method for the calculation of dispersion properties of guided waves in plates

Salah-Eddine HEBAZ, Farouk BENMEDDOUR,*
Emmanuel MOULIN, and Jamal ASSAAD
Univ. Valenciennes, CNRS, Univ. Lille,
YNCREA, Centrale Lille, UMR 8520 - IEMN,
DOAE, F-59313 Valenciennes, France.

(Dated: November 29, 2017)

Abstract

The development of reliable guided waves inspection systems is conditioned by an accurate knowledge of their dispersive properties. The semi-analytical finite element method have been proved very practical for modeling wave propagation in arbitrary cross-section waveguides. However, when it comes to computations on complex geometries to a given accuracy, it still has a major drawback: the high consumption of resources. Recently, Discontinuous Galerkin Finite Element Methods (DG-FEM) has been found advantageous over the standard finite element method when applied as well in the frequency domain. In this work, a high-order method for the computation of Lamb modes characteristics in plates is proposed. The problem is discretised using a class of DG-FEM namely the interior penalty methods family. The analytical validation is performed through the homogeneous isotropic case with traction-free boundary conditions. Afterwards, functionally graded material plates are analysed and a numerical example is presented. It was found that the obtained results are in good agreement with those found in the literature.

PACS numbers: 43.20.Bi, 43.20.Ks, 43.20.Mv, 02.70.Dh, 02.70.-c

* Farouk.Benmeddour@univ-valenciennes.fr; Corresponding author.

I. INTRODUCTION

It is amply admitted that ultrasonic guided waves provide an efficient and rapid means of non-destructive evaluation (NDE) and structural health monitoring (SHM) of a wide range of solid structures. Their increased sensitivity makes it possible to detect early damage over long distances in such a short time. Nevertheless, they have certain complex characteristics (multimodal, dispersion and attenuation) that makes it difficult to analysis, modeling and interpretation. Therefore, a previous knowledge of the wave propagation characteristics is very crucial. On the one hand, they help predict the possible wave propagation features and provide a better understanding of the physical phenomenon. On the other hand, they are of paramount interest to the design and the development of reliable inspection systems. However, these properties are not always accessible analytically, which need the use of numerical methods [1].

Indeed, miscellaneous researches have been carried out to study and modelise the guided waves propagation in different types of structures. Various numerical techniques have been developed to replace the analytic approaches limited to simple case geometries [2], [3]. Classical Finite Elements (FE) based methods have been extensively used [4]. Among others, the Semi-Analytical FE (SAFE) techniques has been demonstrated very practical for extracting dispersion curves and vibration modes of arbitrary cross-section waveguides. It uses the FE discretisation only for the cross-section, hence complex shapes can be handled. The propagation along the guide are described as a harmonic function. Thus, the calculation time is considerably reduced and remain constant regardless of the guide's length (for more details see [5–9]). Over and above, it has been applied to several types of structures like plates, rods, pipelines and railways; for isotropic, composite, anisotropic and dumped media

[10]. The semi-analytical approach has been also modified to deal with bended/curved and periodic plates [11, 12]. Otherwise, its combination with other approaches yields efficient techniques to investigate wave-damage interaction [4, 13]. However, despite the economical scheme of the SAFE technique, computing dispersion curves of some real industrial structures (e.g. railways and pipelines) at relatively high frequencies remain fastidious. The low convergence rate of the conventional FE discretisation impacts the results accuracy and the computational cost [10, 14]. The mesh refinement results in an intensified resource consumption and/or at a certain point a great error causing an inaccurate numerical solution.

Accordingly, computations in high frequency ranges is a major challenge to date.

In fact, the most SAFE formulations in the literature are developed using *hp* low-order FEs usually limited to second order approximations. Although there has been great advances in the use of high-order formulations to achieve high convergence rates, specifically for the guided wave propagation problems [15, 16]. Unfortunately, to the best authors' knowledge, the SAFE methods have surprisingly not benefit from their advantages.

Over the last decade, an ingenious mix of the FE Method (FEM) and the Finite Volume Method (FVM) called the Discontinuous Galerkin FE method (DG-FEM) [17, 18] has been of great interest to many researchers in the field of the wave propagation simulation in the time domain [15, 19–22]. Since it uses the same space of basis functions as the FEM and a local formulation close to the FVM, it enjoys the benefits of both: high-order approximations enabling a coarser mesh to be used while maintaining a high degree of accuracy, naturally parallelisable scheme, etc.

Recently, it has been found in [23] that the DG-FEM is advantageous over the standard FE method when applied to eigenvalue problems; particularly in the oriented wave number calculations like dispersion curves. Accordingly, in this work, a high-order Semi-Analytical Discontinuous Galerkin Finite Element (SADG-FE) method is developed for the one dimensional case. The verification and validation are performed via Lamb modes problem in homogeneous isotropic plates, a case for which theoretical aspects are available and well documented in the literature. Otherwise, by dint of its discontinuous nature, the proposed approach can be used with no change for plate-like structures with continuous varying parameters.

The linear elastic waves equation is formulated in terms of the displacement. Applying the semi-analytic approach, the problem is simplified to a one dimensional ordinary differential system in the through-thickness direction. The second-order operator is then discretised using a class of DG methods namely the Interior Penalty Discontinuous Galerkin methods (IPDG), while the first order operator is approximated by the Standard Discontinuous Galerkin (SDG) method. Taking into account the free boundary conditions, the resulting algebraic system becomes a quadratic eigenvalue problem. By solving the latter, Lamb waves characteristics are obtained and compared to the analytic solutions of the Rayleigh-Lamb frequency equations. Afterwards, a Functionally Graded Material (FGM) example is analysed and compared with results found in the literature [24].

This study is organised as follows: in section (II), the semi-analytical approach and a general description of the Lamb modes problem are presented. Then, the variational formulation of the semi-analytical discontinuous Galerkin method is given. Therewith, in section (III), the implementation details for homogeneous and FGM cases are discussed. Next, the results of the numerical experiments are shown and discussed in section (IV). Finally, a conclusion in section (V) to summarise the main points of the study and its interest to future work.

II. SADG-FE FORMULATION FOR GUIDED WAVES IN PLATES

In this section, the discretisation of the Lamb modes problem by means of discontinuous Galerkin methods is presented. The traction-free boundary conditions are implemented and the eigenvalue problem is constructed.

A. General description of the problem

Consider an elastic isotropic waveguide with a cross-section $\mathbf{S}$ in the (x_1, x_2) plane having an invariance along the propagation axis x_3. The elastic waves are governed by the Navier's displacement equation of motion resulting from the fundamental principle of dynamics [25–27]:

$$(\lambda+\mu)\frac{\partial^2 u_j}{\partial x_j \partial x_i} + \mu\frac{\partial^2 u_i}{\partial x_j^2} + \rho f_i = \rho\frac{\partial^2 u_i}{\partial t^2}, \qquad i,j = 1,2,3 \tag{1}$$

where u_i are the components of the displacement field $\mathbf{u} = [u_1, u_2, u_3]^T$, the superscript T designates transpose. λ and μ are the Lamé coefficients. f_i are the body forces, ρ is the density of the material and t is the time. The Einstein summation convention over repeated indexes is adopted. We emphasize that the parameters are allowed to vary smoothly throughout the thickness.

Looking for solutions in time harmonic domain $\mathbf{u}(\mathbf{x}, t) = \widehat{\mathbf{u}}(\mathbf{x})e^{-i\omega t}$ and under the hypothesis of invariance of the material properties and the geometry of the guide in the direction

111 of propagation x_3, the displacements field can be expressed as:

$$\widehat{\mathbf{u}}(\mathbf{x}) = \mathbf{U}(x_1, x_2)e^{+ikx_3}, \tag{2}$$

112 where k is the wave number and ω is the angular frequency. Consequently, this harmonic
113 function e^{+ikx_3} leads to the separation of the propagation analysis in the cross-section from
114 the rest of the domain.

115

116 Let be an isotropic homogeneous plate of constant thickness $2d$, of infinite lateral dimen-
117 sions and free from any external constraints as shown in Figure (1).

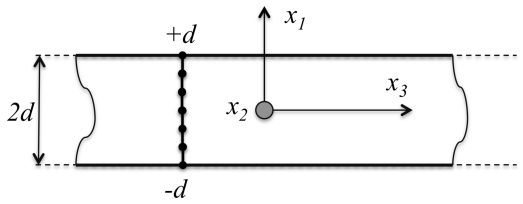

Figure 1. Geometry of the 2-D waveguide in the direction of propagation x_3: isotropic homogeneous plate of thickness $2d$ and infinite lateral dimensions.

118 Unlike a three dimensional (3-D) waveguide for which the resonance occurs in the section
119 and spread in the extrusion direction, the resonance in plates (2-D waveguide) takes place in
120 the thickness. Consequently, the propagation can take place in any direction perpendicular
121 to it since they both have the same invariance. Therefore, by choosing a principal direction
122 of propagation, the study of the phenomenon occurs naturally in its plane with the direc-
123 tion that limits the geometry of the guide, plane (x_1, x_3). This leads us to seek solutions
124 independent of the variable x_2. Hence, the sought solutions are of the form

$$\widehat{\mathbf{u}}(\mathbf{x}) = \mathbf{U}(x_1)e^{+ikx_3}, \tag{3}$$

125 and they are associated with the free surface condition

$$\sigma(\widehat{\mathbf{u}}).\mathbf{e}_1 = 0 \qquad \text{in } x_1 = \pm d. \tag{4}$$

126 Thus, by eliminating the variable x_2 from the system, one obtains the simplified equations
127 for a plate, placed only on a line of the thickness. Substituting (3) in (1), after simplification

and rearrangement, the problem of Lamb modes in the matrix form becomes:

$$\begin{cases} [\mathbf{M}_0]\dfrac{\partial^2 \mathbf{U}_{13}}{\partial x_1^2} + ik[\mathbf{M}_1]\dfrac{\partial \mathbf{U}_{13}}{\partial x_1} \\ \qquad\qquad - (k^2[\mathbf{M}_2] - \omega^2[\mathbf{M}_3])\mathbf{U}_{13} = 0, \\ [\mathbf{M}_0]\dfrac{\partial \mathbf{U}_{13}}{\partial x_1}(\pm d) + ik[\mathbf{M}_4]\mathbf{U}_{13}(\pm d) = 0, \end{cases} \tag{5}$$

with:

$$[\mathbf{M}_0] = \begin{bmatrix} (\lambda+2\mu) & 0 \\ 0 & \mu \end{bmatrix}, \qquad [\mathbf{M}_1] = \begin{bmatrix} 0 & (\lambda+\mu) \\ (\lambda+\mu) & 0 \end{bmatrix},$$
$$[\mathbf{M}_2] = \begin{bmatrix} \mu & 0 \\ 0 & (\lambda+2\mu) \end{bmatrix}, \qquad [\mathbf{M}_3] = \begin{bmatrix} \rho & 0 \\ 0 & \rho \end{bmatrix},$$
$$[\mathbf{M}_4] = \begin{bmatrix} 0 & \lambda \\ \mu & 0 \end{bmatrix}, \qquad \mathbf{U}_{13} = \begin{bmatrix} U_1 & U_3 \end{bmatrix}^T.$$

To analyse the behaviour of the 2-D waveguide, the wave numbers k and the corresponding mode shapes $\mathbf{U}_{13}$ must be found as a function of a given frequency ω or inversely. The pair (ω, k) for which there exist non-trivial solutions describe the called dispersion curves of the vibration modes. The analytic solutions expressions of the dispersion relations $D(\omega, k)$ can be found in several works (see e.g. the classical text books [3, 28, 29]).

Without loss of generality, we will focus on Lamb modes. The dispersion relation for Horizontal Transverse (HT) modes is similar to that of the slender rod (1-D waveguide) already analysed in [23]. Furthermore, we refer to the "exact" Lamb mode solutions k^{ex} as the analytic values obtained using a root tracking method to search the zeros of Rayleigh-Lamb equations for a given frequency range and up to a tolerance of 10^{-16}. The latter will serve as a verification tool to validate the proposed method.

B. Discontinuous variational formulation

The system (5) is defined on the domain $I = [-d, +d]$, a line of the thickness of the plate depicted in Figure (1). For the sake of simplicity, we denote by x the variable x_1 for rest

of the section. As shown in Figure (2), the thickness is partitioned into a finite number of n one-dimensional non-overlapping elements $E_j = [x_j, x_{j+1}]$, where $\{j = 0, .., n-1\}$ is the index of elements. The mesh is allowed to be non uniform. We define the size of each element by: $h_j = x_{j+1} - x_j \quad \text{and} \quad h_{max}(j) = max(h_{j-1}, h_j)$.

The key idea of the DG-FEM is that the weighting functions are chosen in a way that the field variable and its derivatives are considered discontinuous across the boundaries of the element while the continuity of the computational domain is maintained.

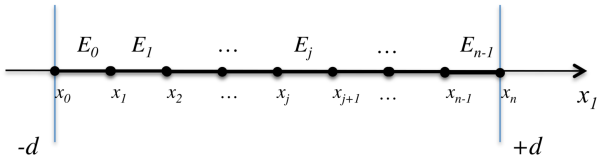

Figure 2. Discretisation of the plate thickness.

Therefore, we denote by $\mathcal{D}_p$ the space of the discontinuous piecewise test-functions $v(x)$ on the mesh $I_h = \bigcup_j E_j$ such as:

$$\mathcal{D}_p(I_h) = \{v : v\mid_{E_j} \in \mathbb{P}_p(E_j) \quad \forall j = 1, .., n-1\},$$

where $\mathbb{P}_p(E_j)$ is the space of interpolation polynomials of order p in the element E_j. It is important to note that for $v\mid_{E_j}$ defined only inside, we write:

$$v(x_j) = v(x_j^+) = \lim_{\substack{\epsilon \to 0 \\ \epsilon > 0}} v(x_j + \epsilon),$$
$$v(x_{j+1}) = v(x_{j+1}^-) = \lim_{\substack{\epsilon \to 0 \\ \epsilon > 0}} v(x_{j+1} - \epsilon).$$

Accordingly, we define the jump $[\![\bullet]\!]$ and average $\{\!\{\bullet\}\!\}$ across the interface between two adjacent elements:

$$\begin{aligned} [\![\cdot]\!] &= (\cdot\mid_L) - (\cdot\mid_R), \\ \{\!\{\cdot\}\!\} &= q_L(\cdot\mid_L) + q_R(\cdot\mid_R), \end{aligned} \tag{6}$$

where q_L and q_R are respectively the coefficients of the average of the element on the left and the right of the considered interface. This definition of the average here is general.

However, in this work we will use the special case where $q_L = q_R = \frac{1}{2}$.

By means of the weighted residuals method, multiplying the first part of (5) by a discontinuous test function $v(x)$ and integrating the result over the cell E_j, the elementary strong integral form is obtained:

$$\int_{x_j}^{x_{j+1}} \Big([\mathbf{M}_0] \frac{\partial^2 \mathbf{U}_{13}}{\partial x^2} + ik[\mathbf{M}_1] \frac{\partial \mathbf{U}_{13}}{\partial x} + (\omega^2 [\mathbf{M}_3] - k^2 [\mathbf{M}_2]) \mathbf{U}_{13} \Big) v \, \mathrm{d}x = 0. \tag{7}$$

In order to simplify the derivation of the DG formulation of the problem (5), we will consider each operator (first and second order derivative) and its discretisation apart. Afterward, we retrieve the general SADG-FE scheme such that: find $\mathbf{U}_{13} \in \mathcal{D}_p(I_h)$

$$\forall v \in \mathcal{D}_p(I_h), \qquad a(\mathbf{U}_{13}, v) = \mathcal{L}(v),$$

where $a(.,.)$ is called the bilinear form and its corresponding right hand, the linear form $\mathcal{L}(.)$.

To begin with, consider the integral of the first-order operator of (7). For clarity reasons let be

$$\mathbf{f}(\mathbf{U}_{13}) = [\mathbf{M}_1] \mathbf{U}_{13}.$$

To obtain the weak integral form, we integrate by parts. We obtain :

$$\begin{aligned} &- \int_{x_j}^{x_{j+1}} \frac{\partial \mathbf{f}(\mathbf{U}_{13})}{\partial x} v \, \mathrm{d}x \\ &= \int_{x_j}^{x_{j+1}} \mathbf{f}(\mathbf{U}_{13}) \, \frac{\partial v}{\partial x} \, \mathrm{d}x - \left[\; \bar{\mathbf{f}} v \; \right]_{x_j}^{x_{j+1}}. \end{aligned} \tag{8}$$

The discontinuous formulation allows the approximated field to be discontinuous across boundaries. Therefore, the solutions at the interfaces are duplicated. A treatment of the inter-element discontinuity is necessary in order to connect the elements and complete the discretisation. The right-hand part $\bar{\mathbf{f}}$ of the jump of (8) is then calculated based on the two

available values

$$\bar{\mathbf{f}} = g(\mathbf{f}_L, \mathbf{f}_R), \tag{9}$$

where $\mathbf{f}_L$ and $\mathbf{f}_R$ are respectively the values of $\mathbf{f}(\mathbf{U})$ at the left and the right of the element interface; g is a linear combination called the numerical flux.

Indeed, various flux formulas allowing to obtain different DG methods for different applications have been developed in the literature [17, 18]. Nevertheless, in this work we consider a more general formula [30]:

$$\bar{\mathbf{f}}(\mathbf{U}_{13}) \mid_{\partial E_j} = \{\!\{\mathbf{f}(\mathbf{U}_{13})\}\!\} + \theta[\![\mathbf{U}_{13}]\!], \tag{10}$$

where θ is a scalar parameter.

So, by making the sum of (8) for all the elements and substituting $\bar{\mathbf{f}}$ by the flux formula (10), the following SDG formulation is obtained:

$$\begin{aligned} a_1(\mathbf{U}_{13}, v) = &\sum_{j=0}^{n-1} \int_{x_j}^{x_{j+1}} \mathbf{f}(\mathbf{U}_{13}) \, \frac{\partial v}{\partial x} \, \mathrm{d}x \\ &- \sum_{j=1}^{n-1} \{\!\{\mathbf{f}(x_j)\}\!\} [\![v(x_j)]\!] - \theta \sum_{j=1}^{n-1} [\![\mathbf{U}_{13}(x_j)]\!] [\![v(x_j)]\!]. \end{aligned} \tag{11}$$

Now, consider the second-order derivative term in (7). In the same way, using Green's theorem yields the weak integral form such that:

$$\begin{aligned} &- \int_{x_j}^{x_{j+1}} \frac{\partial}{\partial x} \left([\mathbf{M}_0] \frac{\partial \mathbf{U}_{13}}{\partial x} \right) v \, \mathrm{d}x \\ &= \int_{x_j}^{x_{j+1}} [\mathbf{M}_0] \frac{\partial \mathbf{U}_{13}}{\partial x} \frac{\partial v}{\partial x} \, \mathrm{d}x - \left[[\mathbf{M}_0] \frac{\partial \bar{\mathbf{U}}_{13}}{\partial x} v \right]_{x_j}^{x_{j+1}}. \end{aligned} \tag{12}$$

In fact, the logic of the previous flux formulation used for the 1^{st} order operator is not entirely applicable in the present case of (12). There exist different DG methods designed for elliptic equations. On the one hand, the mixed formulations consist of rewriting the 2^{nd} order term as a first-order system. On the other hand, a direct straightforward discretisation techniques based on stabilisation methods called the primal formulations. In this work we shall use one of the latter DG methods, namely the Interior Penalty (IP) methods.

By summing up (12) for all the elements, stabilisation terms are then added to the formulation. The first and the second terms correspond to the numerical flux resulting from the integration. The other terms are a penalisation functions which enable to impose a weak continuity of the numerical solution and its derivatives. Hence, the general expression of the interior penalty discontinuous Galerkin approximation of the Laplacian operator becomes:

$$\begin{aligned} a_0(\mathbf{U}_{13}, v) = & \sum_{j=0}^{n-1} \int_{x_j}^{x_{j+1}} [\mathbf{M}_0] \frac{\partial \mathbf{U}_{13}}{\partial x} \frac{\partial v}{\partial x} \, \mathrm{d}x \\ & - \sum_{j=1}^{n-1} \left\{ \left[\mathbf{M}_0 \right] \frac{\partial \mathbf{U}_{13}(x_j)}{\partial x} \right\} \llbracket v(x_j) \rrbracket \\ & + \varepsilon \sum_{j=1}^{n-1} \left\{ \left[\mathbf{M}_0 \right] \frac{\partial v(x_j)}{\partial x} \right\} \llbracket \mathbf{U}_{13}(x_j) \rrbracket \\ & + \sum_{j=1}^{n-1} \frac{\alpha}{h_{max}(j)} \llbracket \mathbf{U}_{13}(x_j) \rrbracket \llbracket v(x_j) \rrbracket \\ & + \sum_{j=1}^{n-1} \frac{\gamma}{h_{max}(j)} \llbracket \frac{\partial \mathbf{U}_{13}(x_j)}{\partial x} \rrbracket \llbracket \frac{\partial v(x_j)}{\partial x} \rrbracket, \end{aligned} \tag{13}$$

where ε, α and γ are real numbers to be adjusted, called penalty factors. There are three cases of ε in the literature $\{-1; 0; +1\}$. In each case, a variant of IP methods can be identified: the Symmetric (SIPDG), Incomplete (IIPDG) and Non-symmetric (NIPDG) derivations. Details of the development and implementation are omitted here, however a more rigorous mathematical analysis and a detailed bibliography are provided in [18, 31].

Note that these forms are not yet complete, the field of border elements, i.e. boundary conditions (BC), are not taken into account yet. The problem is associated with the stress free surface condition in (5): $[\mathbf{M}_0] \frac{\partial \mathbf{U}_{13}}{\partial x_1}(\pm d) + ik[\mathbf{M}_4]\mathbf{U}_{13}(\pm d) = 0$. This is a linear relation between the values of the function and its derivative on the boundaries, a weighted combination of a Dirichlet and a Neumann BCs. It is called Robin boundary conditions.

In the framework of the DG methods, the implementation of BCs remains a delicate task. Unlike the classical FE method, the approximated field is considered discontinuous across the borders and thus we don't have a direct access to it. Several processing techniques have been developed for each type of boundary conditions. Dirichlet BC are usually imposed

weakly through the numerical flux and thus contribute to both left hand and right hand sides. As for Neumann type, their insertion lies in the fact that they directly satisfy the integral on the borders. Hence, it can be moved to the right hand side and makes no contribution to the bilinear form.

In fact, considering the boundary nodes (x_0, x_n), one can easily see that the Dirichlet BC part is naturally obtained by integration by parts in (8) and the Neumann BC in (12), respectively. By summing the two jumps, we obtain:

$$\left[\left([\mathbf{M}_0]\frac{\partial \mathbf{U}_{13}}{\partial x_1} + ik[\mathbf{M}_1]\mathbf{U}_{13}\right) v\right]_{x_0}^{x_n}. \tag{14}$$

However, it still does not totally satisfy the latter condition. Thereby, let be a matrix $[\mathbf{M}_5]$ such that: $[\mathbf{M}_1] = [\mathbf{M}_4] + [\mathbf{M}_5]$. By substituting in (14), we obtain two expressions. The integral matching the BC is moved directly to the right hand

$$\mathcal{L}(v) \quad = \int_{\partial I} \left([\mathbf{M}_0]\frac{\partial \mathbf{U}_{13}}{\partial x_1} + ik[\mathbf{M}_4]\mathbf{U}_{13}\right) v \,\mathrm{d}x, \tag{15}$$

while the other one makes a contribution to the bilinear form:

$$\begin{aligned} a_1(\mathbf{U}_{13}, v) = &\sum_{j=0}^{n-1} \int_{x_j}^{x_{j+1}} \mathbf{f}(\mathbf{U}_{13}) \, \frac{\partial v}{\partial x} \,\mathrm{d}x \\ &- \sum_{j=1}^{n-1} \{\!\{\mathbf{f}(x_j)\}\!\} [\![v(x_j)]\!] \\ &- \theta \sum_{j=1}^{n-1} [\![\mathbf{U}_{13}(x_j)]\!] [\![v(x_j)]\!] \\ &+ \sum_{j=0,n} \{\!\{[\mathbf{M}_5]\mathbf{U}_{13}(x_j)\}\!\} [\![v(x_j)]\!], \end{aligned} \tag{16}$$

where

$$[\mathbf{M}_5] = [\mathbf{M}_1] - [\mathbf{M}_4] = \begin{bmatrix} 0 & \mu \\ \lambda & 0 \end{bmatrix}. \tag{17}$$

Finally, getting all together, the discontinuous scheme is complete. The problem ~~is~~ be-

comes: look for $\mathbf{U}_{13} \in \mathcal{D}_p(I_h)$ such that

$$\forall v \in \mathcal{D}_p(I_h), \qquad a(\mathbf{U}_{13}, v) = 0, \tag{18}$$

where the global bilinear form $a(\mathbf{U}_{13}, v)$ is given by

$$\begin{aligned} a(\mathbf{U}_{13}, v) = a_0(\mathbf{U}_{13}, v) + ik\ a_1(\mathbf{U}_{13}, v) \\ + k^2\ a_2(\mathbf{U}_{13}, v) - \omega^2 a_3(\mathbf{U}_{13}, v), \end{aligned} \tag{19}$$

with

$$a_{i=2,3}(\mathbf{U}_{13}, v) = [\mathbf{M}_{i=2,3}] \sum_{j=0}^{n-1} \int_{x_j}^{x_{j+1}} \mathbf{U}_{13} v \, \mathrm{d}x.$$

Obviously, this is an eigenvalue problem or in k or in ω and U is the associated eigenvector. Non-trivial eigen-solutions can be found either by fixing the frequency to a positive real number ($\omega \in \mathbb{R}^+$) and the problem is solved for the wave number k in the complex plane. Either a real or complex wave number k is given and the resolution is made for ω. In general, the first case is the most used because it allows to study the all types of modes: propagative ($k \in \mathbb{R}$), non-propagative and inhomogeneous ($k \in \mathbb{C}$).

III. IMPLEMENTATION

This section presents a numerical implementation of the SADG-FE method. First, the homogeneous isotropic plate is studied. Afterwards, functionally graded material plates are analysed. Then, a convenient technique to linearise the quadratic eigenvalue problem is described.

A. Homogeneous isotropic plate

The discretisation of the bilinear form by nodal approximation makes it possible to construct the algebraic system. In each cell E_j, the solution is expressed by :

$$U^{(j)}_{i=1,3}(x) = \sum_{l=0}^{p} P_l(x) U^{(j)}_{l_{i=1,3}} = \mathbf{P}\tilde{\mathbf{U}}^{(j)}_{i=1,3}, \tag{20}$$

belonging to the same space $\mathbb{P}_p(E_j)$ as $v = \mathbf{P}^T$; $\{P_l(x), l = 0, 1, ..., p\}$ are the interpolation polynomials of order p. $\tilde{\mathbf{U}}^{(j)}_{i=1,3}$ is the vector of the nodal displacements of the element j corresponding to the field component $U_{i=1,3}$.

Substituting $\mathbf{U}_{13}$ by its approximation (20) in (19) and calculating for all elements, we obtain a quadratic eigenvalue problem (QEP) :

$$\left[\left([\mathbf{A}_0] - \omega^2[\mathbf{A}_3]\right) + ik\ [\mathbf{A}_1] + k^2\ [\mathbf{A}_2]\right] \{\tilde{\mathbf{U}}_{13}\} = 0. \tag{21}$$

where $\{\tilde{\mathbf{U}}_{13}\} = [\tilde{\mathbf{U}}_1 \tilde{\mathbf{U}}_3]^T$ is the global vector of the generalised nodal displacements. $[\mathbf{A}_{i=0,1,2,3}]$ are the global stiffness and mass matrices obtained as:

$$\begin{aligned}
[\mathbf{A}_0] &= \sum_{j=0}^{n-1} \left(\int_{E_j} \frac{\partial \mathbf{P}^T}{\partial x} [\mathbf{M}_0] \frac{\partial \mathbf{P}}{\partial x}\, \mathrm{d}x + \mathbf{\Gamma}^0_j \right), \\
[\mathbf{A}_1] &= \sum_{j=0}^{n-1} \left(\int_{E_j} \frac{\partial \mathbf{P}^T}{\partial x} [\mathbf{M}_1] \mathbf{P}\, \mathrm{d}x + \mathbf{\Gamma}^1_j \right) + [\mathbf{M}_5][\mathbf{B}], \\
[\mathbf{A}_2] &= \sum_{j=0}^{n-1} \int_{E_j} \mathbf{P}^T [\mathbf{M}_2] \mathbf{P}\, \mathrm{d}x, \\
[\mathbf{A}_3] &= \sum_{j=0}^{n-1} \int_{E_j} \mathbf{P}^T [\mathbf{M}_3] \mathbf{P}\, \mathrm{d}x.
\end{aligned}$$

with $\mathbf{\Gamma}^{0,1}_j$ are the elementary flux matrices. $[\mathbf{B}]$ is the contribution matrix of boundary elements having zero values except for the boundary nodal displacements. Note that $[\mathbf{A}_{i=0,1,2,3}]$ are block partitioned complex square matrices of size $\{(2m \times 2m),\ m = n \times (p+1)\}$. The system of $2m$ quadratic equations admits $2 \times 2m$ non-trivial solutions $(k_i, \{\tilde{\mathbf{U}}_{13}\}_i)$; $i = 1, 2, ..., 4m)$.

Otherwise, when we are dealing with constant parameters all-over the domain, a simplified implementation is possible. Only one component is calculated and the global system matrices are deduced such as:

$$
\begin{aligned}
[\mathbf{A}_0] &= [\mathbf{M}_0] \otimes [\mathbf{K}_{g2}], \\
[\mathbf{A}_1] &= [\mathbf{M}_1] \otimes [\mathbf{K}_{g1}] + [\mathbf{M}_5] \otimes [\mathbf{B}], \\
[\mathbf{A}_2] &= [\mathbf{M}_2] \otimes [\mathbf{M}_g], \\
[\mathbf{A}_3] &= [\mathbf{M}_3] \otimes [\mathbf{M}_g].
\end{aligned}
$$

where $\otimes$ denotes the Kronecker product, the matrices $[\mathbf{K}_{g1}]$ and $[\mathbf{K}_{g2}]$ are the stiffness-flux matrices obtained from the discretisation of the first and second order operators, respectively and $[\mathbf{M}_g]$ is the mass matrix.

B. Functionally graded material plates

The developed method in this paper can be used to study FGM materials with no significant change. This can be carried out by only assigning the desired values of the coefficients in the $[\mathbf{M}_{i=0,1,2,3,4}]$ matrices.

Here, we limit the analysis to the simple FGMs, where two different basic materials change from one to the other. The elastic coefficients are expressed as a function of the thickness [32]. Accordingly, following the formulation in [36], a term involving the derivative function of the coefficients is added to the differential system (5). After simplification and rearrangement, the formulation is modified such as :

$$
[\mathbf{A}_1^*] = [\mathbf{A}_1] + [\mathbf{A}_1^{'}],
$$

with

$$
[\mathbf{A}_1^{'}] = \sum_{j=0}^{n-1} \int_{E_j} \mathbf{P}^T [\mathbf{M}_1^{'}] \mathbf{P} \, \mathrm{d}x,
$$

where

$$[\mathbf{M}_1^{'}] = \begin{bmatrix} 0 & \mu^{'} \\ \lambda^{'} & 0 \end{bmatrix}.$$

Note that the added term vanishes automatically whenever the coefficients are constants, on the whole plate level or on the elementary level. The second approach can be used for discontinuously varying parameters plates by considering the variation like a step-wise gradation in each 1D-element.

Remark: We highlight that to avoid numerical instabilities and improve performances, the model parameters must be non-dimensionalised. Dimensionless variables are introduced and the characteristic quantities (ρ, μ) are normalised with respect to the maximum values of their respective functions. The parameter λ is normalised to μ [33]:

$$\begin{cases} \bar{x} = \dfrac{x}{d}, & \bar{I} = [-1, +1], \\ \bar{\rho} = \dfrac{\rho}{\max\ \rho}, & \bar{\mu} = \dfrac{\mu}{\max\ \mu}, \quad \bar{\lambda} = \dfrac{\lambda}{\max\ \mu}. \\ \Omega = \dfrac{\omega d}{\max\ c_T}. \end{cases}$$

For basic FGMs, the quantities are generally normalised relative to the parameters of the first material.

C. Quadratic system reduction

Direct solving of the QEP is a cumbersome and a complicated task. In practice, it is transformed into a generalised linear eigenvalue (GEP) problem with the same eigenvalues using the linearisation methods proposed in [34].

To reduce to a linear system, an additional variable $\tilde{\mathbf{Q}}_{13} = k\ \tilde{\mathbf{U}}_{13}$ is introduced in (21). Accordingly, the following system is obtained:

$$\begin{cases} \tilde{\mathbf{Q}}_{13} - k\ \tilde{\mathbf{U}}_{13} = 0, \\ [\mathbf{A}_{0\omega 3}]\tilde{\mathbf{U}}_{13} + i[\mathbf{A}_1]\tilde{\mathbf{Q}}_{13} + [\mathbf{A}_2]\ k\ \tilde{\mathbf{Q}}_{13} = 0, \end{cases} \tag{22}$$

with

$$[\mathbf{A}_{0\omega 3}] = [\mathbf{A}_0] - \omega^2[\mathbf{A}_3].$$

Factoring by $\tilde{\mathbf{V}} = [\tilde{\mathbf{U}}_{13}\ \tilde{\mathbf{Q}}_{13}]^T$ and multiplying the second line by -1, the system (21) can be rewritten in the generalised linear form:

$$([\mathbf{A}] - k[\mathbf{B}])\,\{\tilde{\mathbf{V}}\} = \mathbf{0}, \tag{23}$$

with

$$\begin{aligned} [\mathbf{A}] &= \begin{bmatrix} 0 & [I_{2m}] \\ -[\mathbf{A}_{0\omega 3}] & -i[\mathbf{A}_1] \end{bmatrix}, \\ [\mathbf{B}] &= \begin{bmatrix} [I_{2m}] & 0 \\ 0 & [\mathbf{A}_2] \end{bmatrix}. \end{aligned} \tag{24}$$

$[\mathbf{I}_s]$ is the identity matrix of order s.

In fact, the linearisation procedure is not unique. There are several forms in the literature. It is important to choose the one that respects the symmetry and/or other structural properties of the quadratic system. This brings us to one of the main assets of the SADG-FE. the system (23) is more interesting due to the block diagonal nature of the mass matrix $[\mathbf{B}]$. On the one hand, it makes it possible to obtain a hermitian matrix and definite positive. An important property when using GEP solvers and for which the algorithms are more robust and converge faster. On the other hand, it preserves the block-diagonal form of the matrix $[\mathbf{A}_2]$. The latter is a very interesting feature since the inverse of $[\mathbf{B}]$, and thus of $[\mathbf{A}_2]$, is the block diagonal matrix built of the inverse of the blocks:

$$[\mathbf{B}^{-1}] = \begin{bmatrix} [I_{2m}] & 0 \\ 0 & [\mathbf{A}_2^{-1}] \end{bmatrix}, \tag{25}$$

with:

$$[\mathbf{A}_2^{-1}] = \begin{pmatrix} [\boldsymbol{\alpha}_0^{-1}] & 0 & \cdots & 0 \\ 0 & [\boldsymbol{\alpha}_1^{-1}] & \cdots & 0 \\ \vdots & \vdots & \ddots & \vdots \\ 0 & 0 & \cdots & [\boldsymbol{\alpha}_{n-1}^{-1}] \end{pmatrix}.$$

These elementary inverse matrices $[\boldsymbol{\alpha}_i^{-1}]$ can be computed independently and then multiplied directly to construct the global dynamic stiffness matrix $[\mathbf{D}_g] = [\mathbf{B}^{-1}\mathbf{A}]$. Consequently, the assembly of the mass matrix $[\mathbf{M}_g]$ is unnecessary. A computation-time expensive operation is spared. Furthermore, the GEP is again reduced to SEP form. Appropriately, the problem (23) becomes:

$$([\mathbf{D}_g] - k\ [\mathbf{I}_{4m}])\ \{\mathbf{U}\} = \mathbf{0}. \tag{26}$$

This transformation, for problems with large numbers of Degrees Of Freedom (DOFs) leads to a significant gain in computation time.

IV. NUMERICAL RESULTS

In order to validate the SADG-FE method, numerical examples are presented in this section. First, the Lamb waves characteristics are computed for a homogeneous plate. The solutions are then compared with the exact ones. Next, a functionally graded material example is analysed and compared with results in the literature. Afterwards, the potential advantages of the method are discussed.

A. Homogeneous plates

1. Generalities

Let a homogeneous isotropic aluminium plate whose properties are given in Table (I). In this table, c_L, c_T and ν are longitudinal celerity, transversal celerity and Poisson coefficient, respectively. The thickness of the plate is meshed into $n = 60$ linear Lagrange elements ($p = 1$) of the same size $h_j = h$. The global bilinear form is used with the penalty factors $\varepsilon = -1$, $\alpha = 30/h$, $\gamma = 0$ and $\theta = 0$ to insure stability. The averaged flux SDG method and

the SIPG method are used. The same configuration holds for the rest of this work. The SEP (26) is solved for a frequency range $f = (0.00 : 0.01 : 1)$ in MHz. Thus, the minimum recommended requirements for a finite element discretisation are met. The meshing criterion for real solutions $\frac{min(\Lambda)}{h} > 10$ where $\Lambda = c_T/f$ is the wavelength, is largely satisfied.

$2d\ (m)$	$c_L\ (m/s)$	$c_T\ (m/s)$	ν
8e-3	6440.8	3125.4	0.346

Table I. Properties of an aluminium plate.

For a given real frequency range ω, the modal deformations and the corresponding wave numbers describing the dispersion relation $k(\omega)$ are obtained. The solutions k can be either real, imaginary or complex numbers. A first post-processing consists in classifying these solutions into propagative modes (k real), non-propagative modes (k imaginary) and inhomogeneous modes (k complex). For the sake of convenience and clarity, only the rightgoing modes (k positive) are presented and the quantities are dimensionless. In what follows, all the presented results are preformed in MATLAB. Also, the interval of the imaginary part is limited to $\{\Im\mathfrak{m}(kd) \in [-5, +5], \forall f\}$ (see [4]).

2. Dispersion properties

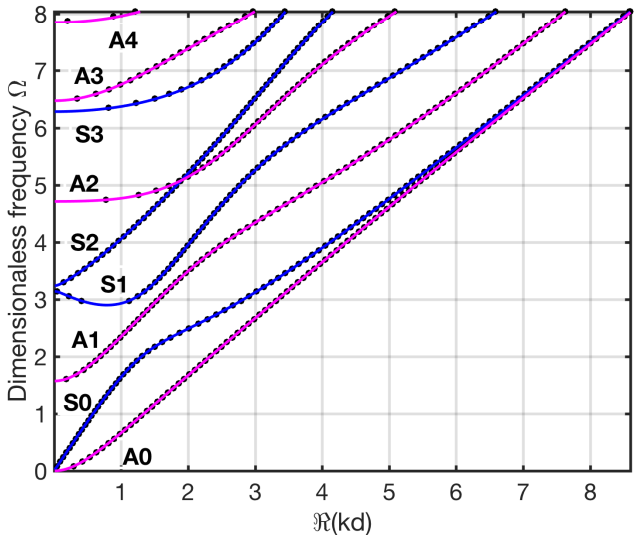

Figure 3. Dispersion curves $D(kd, \Omega)$ of propagative Lamb modes for an isotropic plate: numerical results obtained by the SAFE-DG (black dots) against symmetrical (S) and anti-symmetrical (A) modes of the the analytic solutions plotted in solid blue and red lines, respectively (color online).

The Figure (3) shows the numerical dispersion curves of the SADG-FE (black dots) obtained from the resolution of (26). The figure depicts the dimensionless frequency as a function of the product of the wave number and half-thickness $\Re(kd)$. The results are compared to the exact solutions for the first eight propagative Lamb modes. The analytic curves corresponding to the symmetric modes are plotted with a solid blue lines, while the anti-symmetric modes are represented by solid red lines. A very good agreement is observed.

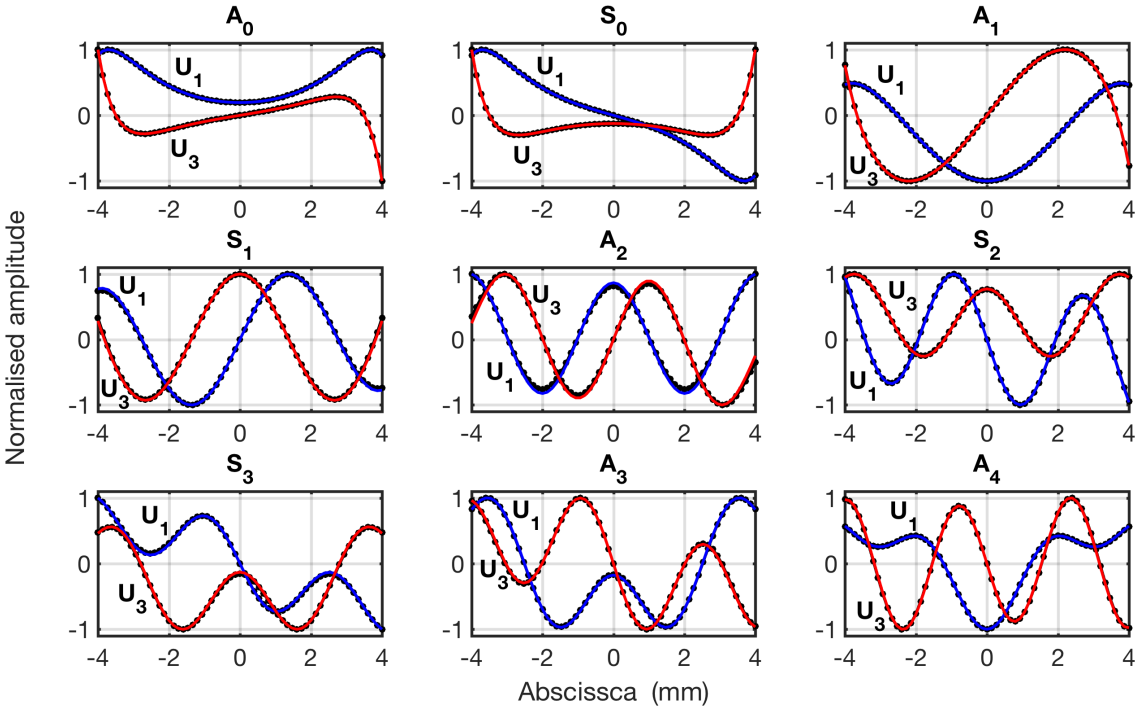

Figure 4. Comparison of numerical results (black dots) against analytical solutions of Lamb mode shapes at the frequency of $1MHz$, $\mathbf{U}_1(x_1)$ and $\mathbf{U}_3(x_1)$ are in blue and red lines, respectively [2] (color online).

To complete the validation of the discontinuous solution, the mode shapes of Lamb modes are compared with analytical ones. The Figure (4) illustrates the discontinuous modal deformations: the profiles of the components $\mathbf{U}_1(x_1)$ and $\mathbf{U}_3(x_1)$ for symmetric and anti-symmetric modes at the frequency of $1MHz$. Each element is plotted independently in a discontinuous manner (black dots). The analytic solutions are plotted in a blue line for the component $\mathbf{U}_1$ and red line for component $\mathbf{U}_3$. The amplitudes are normalised with respect to the maximum. Likewise, a very good match is obtained.

The SADG-FE is now compared to the SAFE method. The Figure (5) shows the complete patterns of inhomogeneous (magenta square and green diamond markers) and non-

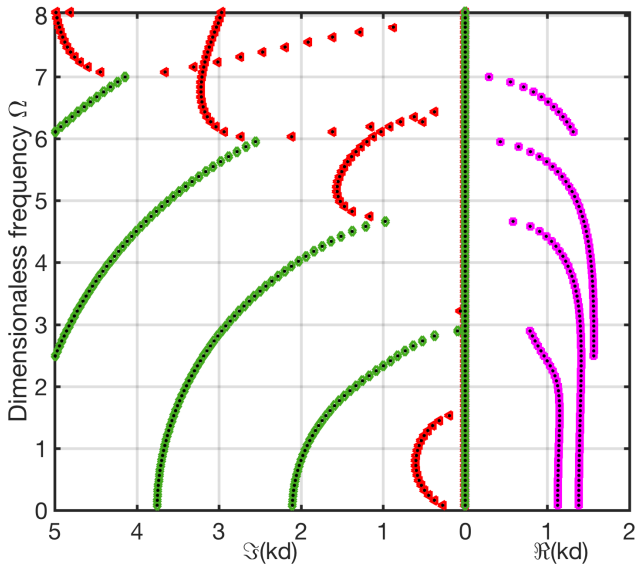

Figure 5. Projection in the complex plane of dispersion curves $D(kd, \Omega)$ of Lamb modes for an isotropic plate: inhomogeneous (magenta square and green diamond markers) and non-propagative (red triangle marker) Lamb modes of the SADG-FE compared to SAFE results (black dots), (color online).

propagative (red triangle marker) Lamb modes (for more details see [35]). Results of the SAFE method are plotted in black dots using the same discretisation. Utterly, the numerical dispersion curves show an excellent agreement. An excelent agreement is also found for the propagative modes. However, results are not shown here for conciseness.

B. Functionally graded materials

In the following, a ceramic-to-chrome material is considered. This FGM was already studied and results are available in the literature [24, 36, 37]. The two isotropic material properties are reported in Table (II).

Material	$\lambda\ (GPa)$	$\mu\ (GPa)$	$\rho\ (kg/m^3)$
chrome	74.2	102.5	7190
ceramic	138	118.11	3900

Table II. Ceramic and chrome properties used for the FGM plate.

The surface ($x = -d$) of the plate is 100% chrome (Cr), while at the other side ($x = +d$)

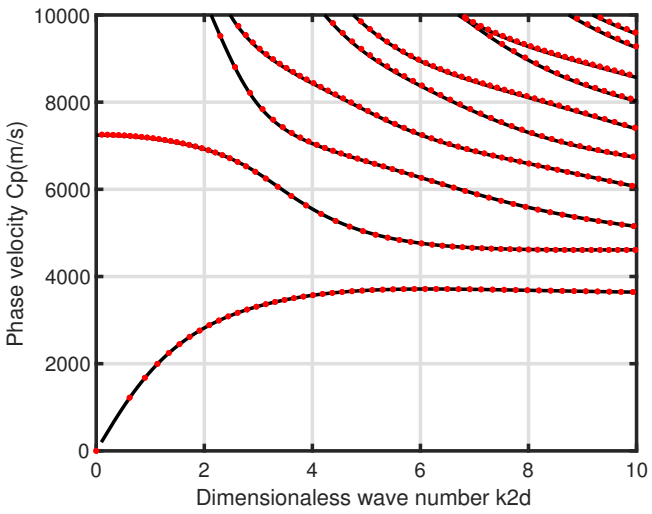

Figure 6. Dispersion curves of the phase velocity C_p of Lamb modes for a FGM isotropic free plate: the SADG-FE numerical results depicted using red dots against the results in [24] plotted in black solid lines. (color online).

the plate is ceramic (Cer). The coefficients through the thickness are expressed as follows:

$$C^{FGM}(x) = \left(C^{Cer} - C^{Cr}\right)\left(\frac{x+d}{2d}\right)^{P_p} + C^{Cr}, \tag{27}$$

where C represents one of the material characteristics (ρ, μ or λ), P_p is a positive integer.

The Figure (6) depicts the obtained dispersion curves of the phase velocity Cp as a function of the dimensionless wave number $k2d$ (red dots). The thickness ($2d = 12e^{-3}\ m$) is partitioned using 90 linear Lagrange elements. The calculations are carried out up to a frequency $f = 3\ MHz$. The quantities are normalised using the chrome parameters. The distribution is taken to be a linear function then $P_p = 1$. In this figure, results are compared to those found in [24] plotted in solid thick lines. The obtained results are in very good concordance.

C. Potential of the SADG-FE method

Many high-order FE formulations for wave propagation simulation are well developed in the literature. Recent comparisons and studies of these methods with respect to their suitability are performed in [16, 22, 38]. Generally, the results have demonstrated their efficiency

when dealing with guided waves and an improved accuracy compared to *hp* low-order FEM. Particularly, the DG-FEM is more advantageous [22, 38]. Firstly, it allows for lower polynomial degree and sampling ratios to be used to get high accuracy. Secondly, it is found more convenient for modeling heterogeneous media. Consequently, the SADG-FE method benefits from the flexibility in treating complex properties, geometries and obtaining an exponential convergence for locally smooth solutions in high frequencies. Thus, handling naturally both interface continuity and free boundary conditions allows very accurate resolutions of guided waves characteristics.

Indeed, the numerical examples presented in this paper are performed only on isotropic materials and using linear Lagrange elements ($p = 1$) with at least ten points to cover the wave length. The obtained results are in excellent agreement with those found in the literature. This constitutes a clear validation of the method, which is the first essential step to further developments dealing with the wave-damage interaction problems [4, 24]. In addition, the proposed approach can be used for any polynomial order and for generally anisotropic multi-layered media as well as axi-symmetric cylinders, since they all deal with the same differential system (5).

The use of higher order polynomials will provide several advantages over the standard method. Indeed, contrary to the continuous Galerkin FEM, precision can be improved by merely increasing the order of polynomials without mesh refinement. The stiffness matrix assembly operations will thus be more efficient and henceforth less time consuming to achieve the same a very good precision.

Moreover, the local mass matrix enables to form directly a standard eigenvalue problem (see section III), instead of a generalised one. This form can be solved more efficiently since there exists many powerful and well suited algorithms, especially for the symmetric case (SIPDG).

Therefore, the developed method has the potential to save a significant computational time both in the assembling and numerical resolution. A precise quantification of these gains necessitates a complete study and is currently in progress.

V. CONCLUSIONS

In this paper, a high-order Semi-Analytical Discontinuous Galerkin Finite Element (SADG-FE) method for the computation of Lamb modes characteristics in plates is presented. The homogeneous isotropic case with free boundary conditions is modeled. Therewith, the extension of the method to functionally graded material plates is shown to be straightforward. Afterwards, numerical results showed that the proposed method provides an excellent agreement with those obtained in the literature. In the aftermath, it was found that the proposed method provides two main features. 1) The algebraic system that can easily and directly transformed into a standard eigenvalue problem, with a partitioned form of elementary blocks well suited for parallelisation, 2) The use of high order elements ($p \geq 3$) can lead to a double gain strategy: the dispersion properties can be computed with fewer elements and thus reducing computational time and achieving high order accuracy.

These properties can gave rise to a high performance tool. Following the conclusions above, the two dimensional wave-guide case is to be developed in a future work.

ACKNOWLEDGMENTS

This research work was supported by The Ministère de l'Enseignement supérieur, de la Recherche et de l'Innovation of France. The authors are grateful to Olivier Bou Matar from IEMN for the very fruitful and constructive discussions.

---

[1] F. Benmeddour, S. Grondel, J. Assaad, and E. Moulin, "Study of the fundamental Lamb modes interaction with symmetrical notches," *NDT & E International*, vol. 41, pp. 1–9, Jan.

2008.

[2] B. A. Auld, *Acoustic fields and waves in solids*, vol. 2. Malabar, Florida: R.E. Krieger publishing company, 2nd ed., 1990.

[3] I. A. Viktorov, *Rayleigh and Lamb waves: physical theory and applications.* New York: Plenum Press, 1967.

[4] F. Benmeddour, F. Treyssède, and L. Laguerre, "Numerical modeling of guided wave interaction with non-axisymmetric cracks in elastic cylinders," *International Journal of Solids and Structures*, vol. 48, pp. 764–774, Mar. 2011.

[5] B. Aalami, "Waves in Prismatic Guides of Arbitrary Cross Section," *Journal of Applied Mechanics*, vol. 40, no. 4, p. 1067, 1973.

[6] P. E. Lagasse, "Higher-order finite-element analysis of topographic guides supporting elastic surface waves," *The Journal of the Acoustical Society of America*, vol. 53, no. 4, p. 1116, 1973.

[7] L. Gavric, "Computation of propagative waves in free rail using a finite element technique," *Journal of Sound and Vibration*, vol. 185, pp. 531–543, Aug. 1995.

[8] A.-C. Hladky-Hennion, "Finite Element analyis of the propagation of acoustic waves in waveguides", *Journal of Sound and Vibration*, vol. 194, pp. 119–136, July 1996.

[9] T. Hayashi, W.-J. Song, and J. L. Rose, "Guided wave dispersion curves for a bar with an arbitrary cross-section, a rod and rail example," *Ultrasonics*, vol. 41, pp. 175–183, May 2003.

[10] I. Bartoli, A. Marzani, F. Lanza di Scalea, and E. Viola. Modeling wave propagation in damped waveguides of arbitrary cross-section. *Journal of Sound and Vibration*, 295(3-5):685–707, Aug. 2006.

[11] F. Treyssde. Elastic waves in helical waveguides. *Wave Motion*, 45(4):457–470, Mar. 2008.

[12] M. V. Predoi, M. Castaings, B. Hosten, and C. Bacon. Wave propagation along transversely periodic structures. *The Journal of the Acoustical Society of America*, 121(4):1935–1944, Apr. 2007.

[13] Z. A. B. Ahmad, J. M. Vivar-Perez, and U. Gabbert. Semi-analytical finite element method for modeling of lamb wave propagation. *CEAS Aeronautical Journal*, 4(1):21–33, Apr. 2013.

[14] F. H. Quintanilla, M. J. S. Lowe, and R. V. Craster. Modeling guided elastic waves in generally anisotropic media using a spectral collocation method. *The Journal of the Acoustical Society of America*, 137(3):1180–1194, Mar. 2015.

[15] O. Bou Matar, P.-Y. Guerder, Y. Li, B. Vandewoestyne, and K. Van Den Abeele, "A nodal

discontinuous Galerkin finite element method for nonlinear elastic wave propagation," *The Journal of the Acoustical Society of America*, vol. 131, pp. 3650–3663, May 2012.

[16] C. Willberg, S. Duczek, J. Vivar Perez, D. Schmicker, and U. Gabbert. Comparison of different higher order finite element schemes for the simulation of Lamb waves. *Computer Methods in Applied Mechanics and Engineering*, 241-244:246–261, Oct. 2012.

[17] B. Cockburn, G. E. Karniadakis, C.-W. Shu, M. Griebel, D. E. Keyes, R. M. Nieminen, D. Roose, and T. Schlick, eds., *Discontinuous Galerkin Methods*, vol. 11 of *Lecture Notes in Computational Science and Engineering*. Berlin, Heidelberg: Springer Berlin Heidelberg, 2000.

[18] D. N. Arnold, F. Brezzi, B. Cockburn, and L. D. Marini, "Unified analysis of discontinuous Galerkin methods for elliptic problems," *SIAM journal on numerical analysis*, vol. 39, no. 5, pp. 1749–1779, 2002.

[19] B. Rivière and M. Wheeler, "Discontinuous Finite Element Methods for Acoustic and Elastic Wave Problems," *Contemporary Mathematics*, vol. 329, pp. 271–282, 2003.

[20] M. Grote, A. Schneebeli, and D. Schotzau, "Discontinuous Galerkin Finite Element Method for the Wave Equation," *SIAM Journal on Numerical Analysis*, vol. 44, pp. 2408–2431, Jan. 2006.

[21] M. Kaser and M. Dumbser, "An arbitrary high-order discontinuous Galerkin method for elastic waves on unstructured meshes - I. The two-dimensional isotropic case with external source terms," *Geophysical Journal International*, vol. 166, pp. 855–877, Aug. 2006.

[22] J. D. De Basabe, M. K. Sen, and M. F. Wheeler, "The interior penalty discontinuous Galerkin method for elastic wave propagation: grid dispersion," *Geophysical Journal International*, vol. 175, pp. 83–93, Oct. 2008.

[23] S. E. Hebaz, F. Benmeddour, E. Moulin, and J. Assad, "Investigating Applicability of Discontinuous Galerkin Methods Towards Structural Health Monitoring in Transportation," in *7th African Conference on Non Destructive Testing (ACNDT 2016)*, (Oran, Algeria), 2016.

[24] F. Benmeddour, E. Moulin, and J. Assaad, "Numerical investigation of the functionally graded materials by the interaction of the plate guided waves with discontinuities and cracks," *The Journal of the Acoustical Society of America*, vol. 133, pp. 3446–3446, May 2013.

[25] B. A. Auld, *Acoustic fields and waves in solids*, vol. 1. Malabar, Florida: R.E. Krieger publishing company, 2nd ed., 1973.

[26] K. F. Graff, *Wave Motion in Elastic Solids*. Courier Corporation, 1975.

[27] J. D. Achenbach, *Wave propagation in elastic solids*. No. 16 in North Holland series in applied mathematics and mechanics, Amsterdam: Elsevier, digital pr ed., 2005.

[28] Raymond D. Mindlin, *The collected papers of Raymond D. Mindlin. Volumes 1 & 2*, vol. 1 & 2. Springer-Verlag, new york, berlin ed., 1989.

[29] J. W. S. Rayleigh, *The theory of sound*. London : Macmillan, 1894.

[30] J. S. Hesthaven and T. Warburton, *Nodal discontinuous Galerkin methods: algorithms, analysis, and applications*. No. 54 in Texts in applied mathematics, New York, NY: Springer, 2008.

[31] B. Rivière, *Discontinuous Galerkin methods for solving elliptic and parabolic equations: theory and implementation*. No. 35 in Frontiers in applied mathematics, Philadelphia, Pa: SIAM, Society for Industrial and Applied Mathematics, 2008.

[32] Y. Miyamoto, *Functionally graded materials: design, processing, and applications*. 1999.

[33] H. P. Langtangen and G. K. Pedersen, *Scaling of Differential Equations*. 2016.

[34] F. Tisseur and K. Meerbergen, "The Quadratic Eigenvalue Problem," *SIAM Review*, vol. 43, pp. 235–286, Jan. 2001.

[35] T. R. Meeker and A. H. Meitzler, "Guided Wave Propagation in Elongated Cylinders and Plates," in *Physical acoustics principles and method*, vol. 1A, pp. 111–167, New York, NY: Academic Press, warren p. mason ed., 1964.

[36] X. Cao, F. Jin, and I. Jeon, "Calculation of propagation properties of Lamb waves in a functionally graded material (FGM) plate by power series technique," *NDT & E International*, vol. 44, pp. 84–92, Jan. 2011.

[37] H. Gravenkamp, C. Song, and J. Prager, "A numerical approach for the computation of dispersion relations for plate structures using the Scaled Boundary Finite Element Method," *Journal of Sound and Vibration*, vol. 331, pp. 2543–2557, May 2012.

[38] M. Ainsworth, P. Monk, and W. Muniz. Dispersive and Dissipative Properties of Discontinuous Galerkin Finite Element Methods for the Second-Order Wave Equation. *Journal of Scientific Computing*, 27(1-3):5–40, June 2006.